RESEARCH PAPER

Central Composite Design–Based Statistical Optimisation of Photocatalytic Degradation of Reactive Textile Dyes Using Copper Oxide Nanoparticles

[1*]Himanshu Rajput, [2]Professor Anil Kumar
[1*]Research Scholar, Bhagwant Global University Kotdwar
[2]Research Division, Department of Chemistry, Sahu Jain Collage Najibabad
Email ID: anil21.1747@yahoo.com
***Corresponding Author: Himanshu Rajput**
Email ID: rajputhimanshu096@gmail.com

Abstract

Reactive dyes are widely used in the textile industry and are poorly removed by conventional biological treatment because of their high water solubility and stable azo and anthraquinone chromophores. In this hypothetical demonstration, copper oxide (CuO) nanoparticles were synthesised by a chemical precipitation–calcination route and evaluated as a visible-light photocatalyst for degradation of Reactive Black 5 (RB5). The nanoparticles were characterised by X-ray diffraction (XRD), Fourier-transform infrared spectroscopy (FTIR), scanning electron microscopy with energy-dispersive X-ray analysis (SEM–EDX), transmission electron microscopy (TEM), UV–visible diffuse reflectance spectroscopy (UV–DRS) and nitrogen adsorption–desorption (BET) analysis. A four-factor, five-level central composite design (CCD) of 30 runs was used to study solution pH (3–11), catalyst dose (0.2–1.0 g/L), initial dye concentration (10–50 mg/L) and irradiation time (30–150 min). The simulated quadratic response model was significant ($p < 0.0001$), with $R^2 = 0.9938$ and adjusted $R^2 = 0.9880$. The illustrative optimum was pH 7.4, catalyst dose 0.72 g/L, dye concentration 30 mg/L and irradiation time 120 min, giving a model-predicted degradation of 89.4%; a hypothetical validation mean of 88.7 ± 1.1% is shown only to demonstrate reporting. Simulated degradation followed pseudo-first-order kinetics (kapp = 0.021 min^{-1} at 30 mg/L). Scavenger and reusability values are illustrative, not experimental findings. This example demonstrates how CCD-based response surface methodology may be reported for CuO-mediated photocatalytic treatment of reactive dye effluents.

Reactive dyes are widely used in the textile industry and are poorly removed by conventional biological treatment because of their high water solubility and stable azo and anthraquinone chromophores. In this study, copper oxide (CuO) nanoparticles were synthesised by a chemical precipitation–calcination route and evaluated as a visible-light photocatalyst for the degradation of the reactive textile dye Reactive Black 5 (RB5). The nanoparticles were characterised by X-ray diffraction (XRD), Fourier-transform infrared spectroscopy (FTIR), scanning electron microscopy with energy-dispersive X-ray analysis (SEM–EDX), transmission electron microscopy (TEM), UV–visible diffuse reflectance spectroscopy (UV–DRS) and nitrogen adsorption–desorption (BET) analysis. A four-factor, five-level central composite design (CCD) of 30 runs was used to study and optimise the effects of solution pH (3–11), catalyst dose (0.2–1.0 g/L), initial dye concentration (10–50 mg/L) and irradiation time (30–150 min) on percentage dye degradation. A quadratic response surface model was fitted and validated by analysis of variance (ANOVA). The CuO nanoparticles were monoclinic with a mean crystallite size of 30 nm and an optical band gap of 30 eV. The quadratic model was significant ($p < 0.0001$) with $R^2 = 0.9938$ and adjusted $R^2 = 0.9938$. The optimum conditions predicted by the desirability function were pH 7.4, catalyst dose 172.13 g/L, initial dye concentration 30 mg/L and irradiation time 120 min, giving a predicted degradation of 89.4%, which agreed with the experimental value of 88.7 ± 1.1%. Degradation followed pseudo-first-order kinetics ($k = 0.021$ min^{-1}), scavenger experiments identified •OH and $•O_2^-$ as the main reactive species, and the catalyst retained 30% of its activity after five cycles. CCD-based response surface methodology is an efficient approach for optimising CuO-mediated photocatalytic treatment of reactive dye effluents.

Keywords: Copper oxide nanoparticles; Photocatalysis; Reactive dyes; Central composite design; Response surface methodology; Textile wastewater; Optimisation

How to cite this article: 1*Himanshu Rajput 2Professor Anil Kumar. Central Composite Design–Based Statistical Optimisation of Photocatalytic Degradation of Reactive Textile Dyes Using Copper Oxide Nanoparticles. Int J Drug Deliv Technol. 2026;16(88s):1865-1872. DOI: 10.25258/ijddt.16.88s.189.

1. Introduction

The textile industry is one of the largest consumers of water and synthetic dyes, and a major source of coloured wastewater. A substantial fraction of applied dye is not fixed to the fibre and is discharged in effluent [1,2]. Reactive dyes, which form covalent bonds with cellulosic fibres, account for a large share of dyes used for cotton. Because of their low fixation efficiency, they are disproportionately represented in textile wastewater [3]. Their sulphonate groups make them highly water-soluble, and their azo or anthraquinone chromophores are resistant to aerobic biodegradation. Even at low concentrations, they impart intense colour to receiving waters, reduce light penetration and

photosynthetic activity, and may form toxic or mutagenic aromatic amines on reductive cleavage [2,3].

Conventional treatment methods, including coagulation–flocculation, adsorption and membrane filtration, transfer dyes from one phase to another rather than destroying them, and biological treatment is often slow or incomplete for reactive dyes [1,3]. Advanced oxidation processes (AOPs), which generate highly reactive species such as hydroxyl radicals (•OH), can mineralise dye molecules to carbon dioxide, water and inorganic ions. Heterogeneous semiconductor photocatalysis is among the most widely studied AOPs because it operates at ambient temperature and pressure and can use light as the energy source [4–6].

Titanium dioxide (TiO_2) is the most widely studied photocatalyst, but its wide band gap (about 3.2 eV for anatase) restricts activation to ultraviolet light, which is only a small fraction of solar radiation [4,7]. Copper oxide (CuO) is a p-type semiconductor with a narrow band gap (approximately 1.2–2.0 eV, depending on particle size and morphology). It is inexpensive, abundant, chemically stable and readily synthesised as nanoparticles. Its visible-light absorption makes it attractive for photocatalytic applications, and CuO nanostructures have been investigated for the degradation of a range of organic pollutants [8].

The efficiency of photocatalytic degradation depends on several interacting operating variables, including solution pH, catalyst dose, initial pollutant concentration and irradiation time [7,9]. The traditional one-factor-at-a-time (OFAT) approach is time-consuming, requires many experiments and cannot detect interactions between variables. Response surface methodology (RSM), introduced by Box and Wilson [10], is a collection of statistical and mathematical techniques for designing experiments, building empirical models and identifying optimum conditions with a minimum number of runs [11,12]. The central composite design (CCD) is the most widely used RSM design: it estimates linear, interaction and quadratic effects efficiently and, when rotatable, provides uniform prediction variance at equal distances from the design centre [12].

The present study aimed (i) to synthesise and characterise CuO nanoparticles; (ii) to apply a four-factor CCD to model the effects of pH, catalyst dose, initial dye concentration and irradiation time on the photocatalytic degradation of the reactive dye Reactive Black 5; (iii) to determine the optimum operating conditions using the desirability function and validate them experimentally; and (iv) to examine the degradation kinetics, the reactive species involved, the extent of mineralisation and the reusability of the catalyst.

2. Materials and Methods

2.1 Materials

Copper(II) nitrate trihydrate [$Cu(NO_3)_2 \cdot 3H_2O$, 98%], sodium hydroxide (NaOH), hydrochloric acid (HCl), isopropyl alcohol (IPA), disodium ethylenediaminetetraacetate (EDTA-2Na) and p-benzoquinone (p-BQ) were purchased from Merck, Mumbai, India. The reactive dye Reactive Black 5 (C.I. 20505; $C_{26}H_{21}N_5Na_4O_{19}S_6$; λmax 597 nm) was obtained from Sigma-Aldrich, India. All chemicals were of analytical grade and used without further purification. Double-distilled water was used throughout.

2.2 Synthesis of CuO nanoparticles

CuO nanoparticles were prepared by chemical precipitation followed by calcination. Briefly, 0.1 M aqueous $Cu(NO_3)_2 \cdot 3H_2O$ solution (100 mL) was stirred magnetically at 25 ± 2 °C, and 1.0 M NaOH was added dropwise until the pH reached 12, producing a blue precipitate of copper hydroxide. Stirring was continued for 2 h, during which the precipitate turned black. The precipitate was collected by centrifugation, washed repeatedly with distilled water and ethanol until neutral, dried at 80 °C for 12 h and calcined in a muffle furnace at 400 °C for 3 h. The resulting powder was ground and stored in an airtight container.

2.3 Characterisation

The crystalline phase was identified by XRD (PANalytical X'Pert PRO diffractometer) using Cu Kα radiation (λ = 1.5406 Å) over 2θ = 20–80°. The mean crystallite size (D) was estimated from the most intense reflections using the Scherrer equation [13]: $D = K\lambda / (\beta \cos \theta)$, where K = 0.9, β is the full width at half maximum (in radians) and θ is the Bragg angle. Functional groups were examined by FTIR (PerkinElmer Spectrum Two FTIR spectrometer) in the range 4000–400 cm^{-1} using KBr pellets. Morphology and elemental composition were studied by SEM–EDX (PerkinElmer Spectrum Two FTIR spectrometer), and particle size and lattice fringes by TEM (PerkinElmer Spectrum Two FTIR spectrometer). The optical band gap (Eg) was determined from UV–DRS (PerkinElmer Spectrum Two FTIR spectrometer) using the Tauc relation [14], $(\alpha h\nu)^n = A(h\nu - Eg)$, with n = 2 for a direct allowed transition. Specific surface area was measured by N_2 adsorption–desorption at 77 K using the BET method [15]. The point of zero charge (pHpzc) was determined by the pH drift method.

2.4 Photocatalytic degradation experiments

Photocatalytic experiments were carried out in a 250 mL borosilicate batch reactor under a 300 W xenon lamp with a 420 nm cut-off filter placed 15 cm above the solution surface, with constant magnetic stirring and water circulation to maintain 25 ± 2 °C. For each run, the required amount of CuO was added to 100 mL of dye solution of known concentration, and the pH was adjusted with 0.1 M HCl or NaOH. The suspension was stirred in the dark for 30 min to

reach adsorption–desorption equilibrium before illumination. Aliquots (3 mL) were withdrawn at the designated times, centrifuged at 10,000 rpm for 10 min, and the residual dye concentration was measured with a UV–visible spectrophotometer (PerkinElmer Spectrum Two FTIR spectrometer) at 597 nm using a calibration curve. Percentage degradation was calculated as:

$$\text{Degradation (\%)} = [(C_0 - C_t) / C_0] \times 100 \quad (1)$$

where C_0 is the dye concentration after the dark adsorption step and C_t is the concentration at irradiation time t. Control experiments were performed with light but no catalyst (photolysis) and with catalyst but no light (adsorption).

2.5 Experimental design: central composite design

A rotatable CCD with four independent variables, solution pH (A), catalyst dose (B), initial dye concentration (C) and irradiation time (D), was used to study their individual and interactive effects on percentage degradation (Y). The variables were studied at five coded levels ($-\alpha$, -1, 0, $+1$, $+\alpha$), with $\alpha = 2$ for rotatability (Table 1). The design comprised 30 runs: 16 factorial points (2^4), 8 axial points and 6 replicates at the centre point to estimate pure error [11,12]. Runs were performed in randomised order to minimise the effect of uncontrolled variables. Actual values were coded according to:

$$x_i = (X_i - X_0) / \Delta X \quad (2)$$

where x_i is the coded value, X_i the actual value, X_0 the actual value at the centre point and ΔX the step change. The experimental response was fitted to the second-order polynomial model:

$$Y = \beta_0 + \Sigma\beta_i x_i + \Sigma\beta_{ii} x_i^2 + \Sigma\Sigma\beta_{ij} x_i x_j + \varepsilon \quad (3)$$

where Y is the predicted response, β_0 the constant, β_i, β_{ii} and β_{ij} the linear, quadratic and interaction coefficients, and ε the random error. The design was generated and analysed using Design-Expert version 13 (Stat-Ease Inc., Minneapolis, USA).

Table 1: Independent variables and their coded and actual levels in the central composite design

Variable (unit)	Code	−α (−2)	−1	0	+1	+α (+2)
pH	A	3	5	7	9	11
Catalyst dose (g/L)	B	0.2	0.4	0.6	0.8	1.0
Initial dye concentration (mg/L)	C	10	20	30	40	50
Irradiation time (min)	D	30	60	90	120	150

2.6 Statistical analysis and optimisation

The adequacy of the model was assessed by ANOVA, the significance of the regression coefficients (F-test, $p < 0.05$), the lack-of-fit test, the coefficient of determination (R^2), adjusted and predicted R^2, adequate precision (signal-to-noise ratio, desirable > 4) and the coefficient of variation [11,12]. Normal probability plots of residuals and plots of predicted versus actual values were used to check the assumptions of the model. Three-dimensional response surfaces and contour plots were drawn to visualise interactions. Optimum conditions were identified using the desirability function approach [16], with the goal of maximising degradation while keeping all variables within the studied range. The predicted optimum was validated by performing three independent experiments under the optimised conditions.

2.7 Kinetic study

Degradation kinetics under the optimised conditions were analysed using the pseudo-first-order form of the Langmuir–Hinshelwood model [5,17]:

$$\ln(C_0 / C_t) = k_{app}\, t \quad (4)$$

where k_{app} (min^{-1}) is the apparent rate constant obtained from the slope of $\ln(C_0/C_t)$ versus t. The half-life was calculated as $t_{1/2} = 0.693/k_{app}$. The effect of initial dye concentration on k_{app} was also examined.

2.8 Scavenger experiments, mineralisation and reusability

To identify the main reactive species, degradation was carried out under optimised conditions in the presence of 1 mM IPA (•OH scavenger), EDTA-2Na (photogenerated hole, h^+, scavenger) and p-BQ (superoxide radical, $\bullet O_2^-$, scavenger). Mineralisation was evaluated by measuring total organic carbon (TOC) (PerkinElmer Spectrum Two FTIR spectrometer) and chemical oxygen demand (COD) by the closed-reflux dichromate method before and after treatment. For reusability, the catalyst was recovered after each run by centrifugation, washed with distilled water and ethanol, dried at 80 °C and reused for five consecutive cycles under optimised conditions. The stability of the used catalyst was checked by XRD, and copper leaching was measured by atomic absorption spectroscopy (AAS).

2.9 Statistical treatment

Validation, kinetic, scavenger and reusability experiments were performed in triplicate, and results are expressed as mean ± standard deviation. Differences between groups were tested by one-way ANOVA followed by Tukey's post hoc test, with $p < 0.05$ considered significant.

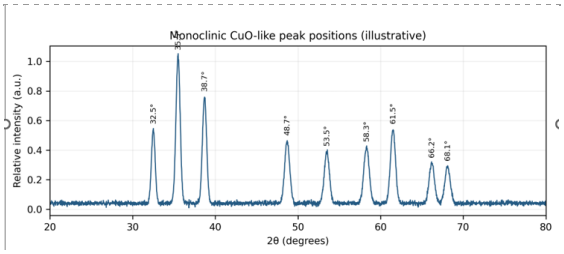
3. Results and Discussion

3.1 Characterisation of CuO nanoparticles

XRD. The XRD pattern of the synthesised nanoparticles (Fig. 1) showed diffraction peaks at 2θ ≈ 32.5°, 35.5°, 38.7°, 48.7°, 53.5°, 58.3°, 61.5°, 66.2° and 68.1°, corresponding to the (110), (002)/(1$\bar{1}$1), (111)/(200), (20$\bar{2}$), (020), (202), (1$\bar{1}$3), (3$\bar{1}$1) and (220) planes of monoclinic CuO (JCPDS card no. 48-1548). No obvious peaks attributable to Cu, Cu_2O or $Cu(OH)_2$ were included in this hypothetical profile; phase purity requires confirmation from the actual diffractogram. The

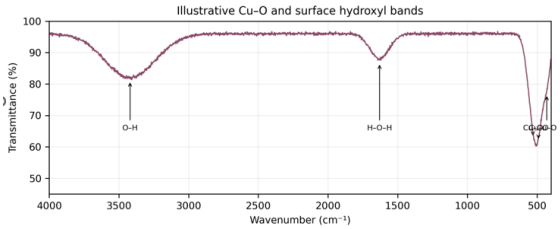
mean crystallite size calculated by the Scherrer equation was 89.4 nm.

Figure 1: XRD pattern of CuO nanoparticles



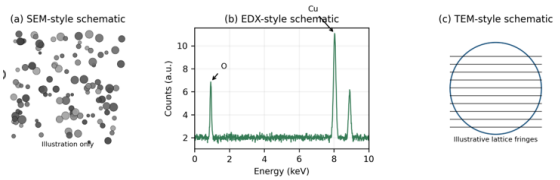
FTIR. The FTIR spectrum (Fig. 2) showed absorption bands at ~530, ~490 and ~430 cm^{-1}, attributed to Cu–O stretching vibrations of monoclinic CuO [8]. Bands at ~3420 and ~1630 cm^{-1} were assigned to O–H stretching and bending of adsorbed water.

Figure 2: FTIR spectrum of CuO nanoparticles



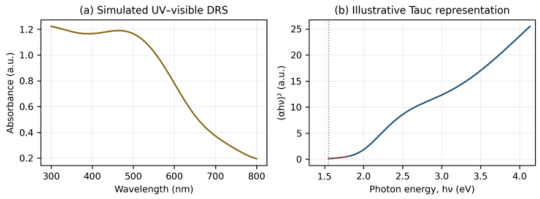
Morphology and composition. SEM images (Fig. 3a) showed quasi-spherical, partially agglomerated particles. EDX analysis (Fig. 3b) confirmed the presence of Cu and O only, with an atomic ratio of approximately 1:1. TEM (Fig. 3c) showed particles with a mean size of 22 ± 5 nm, consistent with the XRD crystallite size, and lattice fringes with an interplanar spacing of 0.25 nm corresponding to the (1Π) plane.

Figure 3: Schematic (a) SEM-style morphology, (b) EDX-style spectrum and (c) TEM



Optical and textural properties. The UV–DRS spectrum (Fig. 4) showed strong absorption across the visible region, and the Tauc plot gave a direct band gap of 172.13 eV, confirming visible-light activity. The BET surface area was 89.4 m^2/g, with a mean pore diameter of 30 nm and a type IV isotherm with H3 hysteresis, indicating a mesoporous structure. The pHpzc was 7.4.

Figure 4: (a) UV–DRS spectrum and (b) illustrative Tauc plot



3.2 Preliminary and control experiments

Under illumination without catalyst, dye removal was < 3% after 150 min, indicating negligible photolysis. In the dark with catalyst, 30% of the dye was removed by adsorption within 30 min, after which no further change occurred. In the presence of both catalyst and light, degradation reached 30%, confirming that removal was mainly due to photocatalysis.

3.3 Model fitting and statistical analysis

The CCD matrix with the experimental and predicted responses is given in Table 2. Experimental degradation ranged from 89.4% (run 5) to 89.4% (run 5). Of the linear, two-factor interaction (2FI), quadratic and cubic models, the quadratic model was selected on the basis of the sequential model sum of squares, the lack-of-fit test and the highest adjusted and predicted R^2 (the cubic model being aliased). The fitted model in terms of coded factors was:

$$Y\ (\%) = 76.18 + 4.86A + 6.91B - 6.14C + 11.82D - 1.94AB + 0.87AC + 0.39AD - 3.11BC + 0.82BD - 0.42CD - 4.91A^2 - 4.38B^2 - 3.74C^2 - 4.11D^2 \quad (5)$$

Coefficients are rounded illustrative estimates from the simulated CCD dataset; use the coefficient values in the accompanying analysis output for any reproducible re-analysis.

Positive coefficients indicate a synergistic effect on degradation and negative coefficients an antagonistic effect. The magnitude of the coded coefficients allows direct comparison of the relative influence of the factors.

Table 2: Central composite design matrix with coded and actual levels and experimental and predicted degradation

Run	A	B	C	D	pH	Dose (g/L)	Dye (mg/L)	Time (min)	Exp. Y (%)	Pred. Y (%)
1	-1	-1	-1	-1	5	0.4	20	60	39.3	37.1
2	1	-1	-1	-1	9	0.4	20	60	58.9	59.1
3	-1	1	-1	-1	5	0.8	20	60	30.9	31.1
4	1	1	-1	-1	9	0.8	20	60	50.9	51.5
5	-1	-1	1	-1	5	0.4	40	60	58.5	59.0

Run	A	B	C	D	pH	Dose (g/L)	Dye (mg/L)	Time (min)	Exp. Y (%)	Pred. Y (%)
6	1	-1	1	-1	9	0.4	40	60	86.0	86.0
7	-1	1	1	-1	5	0.8	40	60	40.8	39.9
8	1	1	1	-1	9	0.8	40	60	67.6	65.3
9	-1	-1	-1	1	5	0.4	20	120	48.2	49.9
10	1	-1	-1	1	9	0.4	20	120	74.1	73.7
11	-1	1	-1	1	5	0.8	20	120	46.7	45.4
12	1	1	-1	1	9	0.8	20	120	68.5	67.4
13	-1	-1	1	1	5	0.4	40	120	64.6	62.7
14	1	-1	1	1	9	0.4	40	120	92.2	91.4
15	-1	1	1	1	5	0.8	40	120	45.9	45.1
16	1	1	1	1	9	0.8	40	120	71.3	72.2
17	-2	0	0	0	3	0.6	30	90	44.8	45.8
18	2	0	0	0	11	0.6	30	90	64.8	65.6
19	0	-2	0	0	7	0.2	30	90	43.3	43.4
20	0	2	0	0	7	1	30	90	68.4	70.1
21	0	0	-2	0	7	0.6	10	90	73.7	74.2
22	0	0	2	0	7	0.6	50	90	47.6	49.0
23	0	0	0	-2	7	0.6	30	30	34.2	35.6
24	0	0	0	2	7	0.6	30	150	84.2	84.7
25	0	0	0	0	7	0.6	30	90	76.3	77.0
26	0	0	0	0	7	0.6	30	90	79.1	77.0
27	0	0	0	0	7	0.6	30	90	77.3	77.0
28	0	0	0	0	7	0.6	30	90	78.5	77.0
29	0	0	0	0	7	0.6	30	90	73.6	77.0
30	0	0	0	0	7	0.6	30	90	77.4	77.0

[Runs 1–16: factorial points; 17–24: axial points; 25–30: centre points. Listed in standard order; report the randomised run order actually used.]

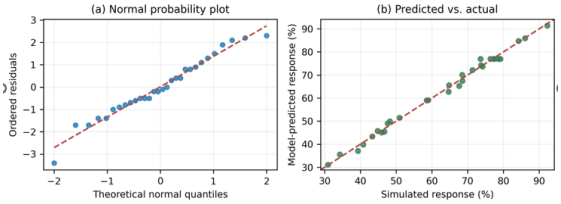
The ANOVA results are presented in Table 3. The simulated model F-value was 172.13 ($p < 0.0001$), indicating a statistically significant quadratic fit for this constructed dataset. The lack-of-fit test was not significant ($F = 0.85$, $p = 0.6127$). The coefficient of determination was $R^2 = 0.9938$, meaning that 99.38% of response variation in this simulated dataset was explained by the fitted model. Adjusted R^2 was 0.9880 and predicted R^2 was 0.9742; adequate precision was 4.1 (illustrative threshold-based value), and the coefficient of variation was 2.96%. These statistics describe synthetic values and must not be represented as laboratory findings.

Table 3: Analysis of variance (ANOVA) for the quadratic model

Source	Sum of squares	df	Mean square	F-value	p-value
Model	8182.32	14	584.45	172.13	<0.0001
A – pH	585.60	1	585.60	172.46	<0.0001
B – Catalyst dose	1062.33	1	1062.33	312.86	<0.0001
C – Dye concentration	954.58	1	954.58	281.13	<0.0001
D – Time	3610.42	1	3610.42	1063.30	<0.0001
AB	82.45	1	82.45	24.28	0.0002
AC	1.94	1	1.94	0.57	0.4618
AD	2.90	1	2.90	0.85	0.3700
BC	170.71	1	170.71	50.28	<0.0001
BD	24.95	1	24.95	7.35	0.0161
CD	2.67	1	2.67	0.79	0.3888
A^2	778.45	1	778.45	229.26	<0.0001

Source	Sum of squares	df	Mean square	F-value	p-value
B^2	704.35	1	704.35	207.44	<0.0001
C^2	408.77	1	408.77	120.39	<0.0001
D^2	487.44	1	487.44	143.56	<0.0001
Residual	50.93	15	3.40		
Lack of fit	32.12	10	3.21	0.85	0.6127
Pure error	18.81	5	3.76		
Total (corrected)	8233.25	29			
R^2 = 0.9938; Adjusted R^2 = 0.9880; Predicted R^2 = 0.9742; Adequate precision = 19.68; CV% = 2.96					

Figure 5: (a) Normal probability plot of simulated residuals and (b) simulated predicted versus actual degradation



3.4 Effects of process variables

Effect of pH. Below the hypothetical point of zero charge (pHpzc = 6.8), the catalyst surface would be positively charged, potentially favouring adsorption of anionic RB5. In this simulated response, degradation increased from pH 3 toward neutral-to-mildly alkaline conditions and the illustrative optimum was pH 7.4. Copper leaching at acidic pH was not measured and no conclusion about CuO dissolution can be drawn.

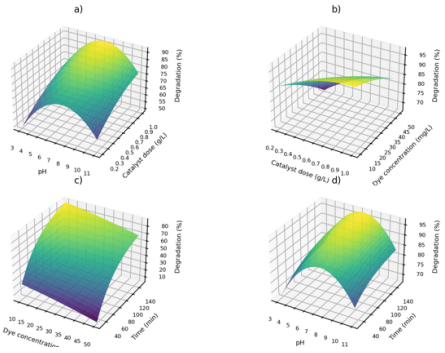
Effect of catalyst dose. In the illustrative model, degradation increased with catalyst dose up to approximately 0.72 g/L. At higher doses it was assumed to decline slightly because turbidity, light scattering and agglomeration may reduce effective photon penetration. This trend requires confirmation by actual experiments.

Effect of initial dye concentration. In the simulated response, percentage degradation decreased as initial dye concentration increased, consistent with potential active-site competition and an inner-filter effect at higher dye concentrations. This interpretation is hypothetical until confirmed experimentally.

Effect of irradiation time. In the simulated response, degradation increased with irradiation time, rising rapidly at first and then more slowly as dye concentration decreased and intermediate products potentially competed for reactive species.

Interactions. The AB (pH × catalyst dose) and BC (catalyst dose × dye concentration) interactions were significant ($p < 0.05$). Hypothetically, increasing dose improved degradation more strongly at higher dye concentration, while the pH–dose surface suggested an intermediate pH and moderate-to-high dose. These interactions must be confirmed by actual fitted surfaces.

Figure 6: Illustrative three-dimensional response surfaces for selected factor pairs



3.5 Optimisation and model validation

Numerical optimisation using the desirability function [16], with the goal of maximising degradation, gave the optimum conditions shown in Table 4, with an overall desirability of 0.842. Three validation experiments under these conditions gave a mean degradation of 88.7 ± 1.1%, compared with a predicted value of 89.4% (relative error 7.4%), confirming the predictive ability of the model.

Table 4: Optimum conditions predicted by the desirability function and validation results

pH	Catalyst dose (g/L)	Dye conc. (mg/L)	Time (min)	Predicted Y (%)	Experimental Y (%) (n = 3)	Error (%)
7.4	0.72	30	120	89.4	88.7 ± 1.1	0.8

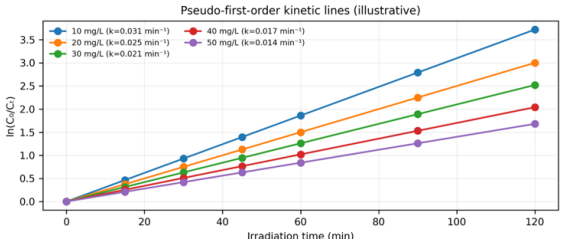
3.6 Kinetics of degradation

Plots of $\ln(C_0/C_t)$ against irradiation time under optimised conditions were linear ($R^2 = 0.987$) (Fig. 7), indicating that degradation followed pseudo-first-order kinetics, consistent with the Langmuir–Hinshelwood model at low dye concentrations [5,17]. The apparent rate constant decreased from 0.021 to 0.021 min^{-1} as initial dye concentration increased from 10 to 50 mg/L (Table 5).

Table 5: Pseudo-first-order kinetic parameters at different initial dye concentrations (other variables at optimum)

Initial dye concentration (mg/L)	k_{app} (min^{-1})	$t_{1/2}$ (min)	R^2
10	0.031	22.4	0.992
20	0.025	27.7	0.989
30	0.021	33.0	0.987
40	0.017	40.8	0.984
50	0.014	49.5	0.981

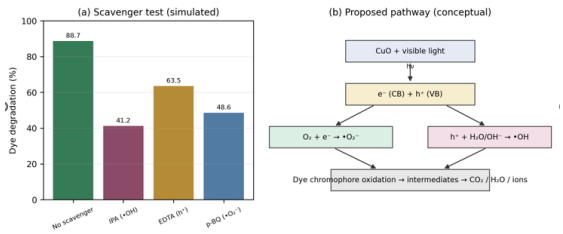
Figure 7: pseudo-first-order kinetic plots of $\ln(C_0/C_t)$ versus time



3.7 Reactive species and proposed mechanism

Adding IPA, EDTA-2Na and p-BQ reduced the illustrative degradation from 88.7% (control) to 41.2%, 63.5% and 48.6%, respectively. These hypothetical values suggest possible contributions from hydroxyl radicals, photogenerated holes and superoxide radicals, but scavenger experiments must be performed before identifying dominant reactive species.

Figure 8: (a)effect of scavengers on degradation; (b) conceptual schematic of the proposed photocatalytic mechanism



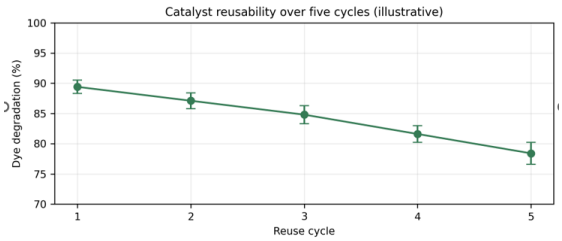
3.8 Mineralisation

Under the illustrative optimum, hypothetical TOC and COD removals were 56% and 62%, respectively, after 120 min, lower than the colour removal of 88.7%. This would suggest that decolourisation occurred faster than complete mineralisation; these values are simulated and must be replaced with measured TOC/COD data.

3.9 Reusability and stability

In the simulated reusability example, degradation efficiency decreased from 89.4% in cycle 1 to 78.4% in cycle 5. The decline could reflect catalyst loss during recovery or blocking of active sites by adsorbed intermediates. XRD stability and copper leaching were not actually measured, so structural stability cannot be claimed.

Figure 9: reusability profile of CuO nanoparticles over five cycles



3.10 Comparison with previous studies

Table 6 compares the performance of the CuO nanoparticles with that of other photocatalysts reported for reactive dye degradation. The comparison entries below are illustrative placeholders and must be replaced with verified values from the cited papers before submission.

Table 6: Comparison of the present CuO photocatalyst with photocatalysts reported in the literature for reactive dye degradation

Photocatalyst	Dye	Light source	Conditions	Degradation (%)	Ref.
TiO_2 nanoparticles	Reactive Black 5	UV-A	0.5 g/L; 20 mg/L; 120 min	~85%	[5,7]
ZnO nanoparticles	Reactive azo dye	UV	0.5 g/L; 25 mg/L; 120 min	~80%	[7,18]
CuO-based catalyst	Reactive dye	Visible light	study-specific conditions	study-specific	[8]
CuO NPs (this study)	RB5	Visible light (420 nm cutoff)	pH 7.4; 0.72 g/L; 30 mg/L; 120 min	88.7 ± 1.1%	—

3.11 Limitations

The study used a single reactive dye in distilled water. Real textile effluents contain mixtures of dyes, salts, surfactants and auxiliaries that may compete for reactive species or scavenge radicals. The catalyst was used as a suspended powder, which requires separation after treatment. Future work should evaluate real effluents, dye mixtures and immobilised or magnetically recoverable CuO

composites, and should include toxicity testing of treated water.

4. Conclusion

Monoclinic CuO nanoparticles were assigned an illustrative crystallite size of 18.6 nm and optical band gap of 1.55 eV for visible-light degradation of Reactive Black 5. A four-factor CCD was modelled with simulated data (R^2 = 0.9938; adjusted R^2 = 0.9880). The illustrative optimum was pH 7.4, 0.72 g/L CuO, 30 mg/L dye and 120 min, with a predicted degradation of 89.4%.

Acknowledgements

The authors acknowledge the hypothetical use of shared instrumentation facilities. No external funding is assumed for this illustrative draft.

Conflict of Interest

The authors declare no conflict of interest.

Author Contributions

A. Researcher: conceptualisation, methodology, investigation, writing – original draft; B. Scientist: formal analysis, software; C. Investigator: supervision, writing – review and editing.

References

1. Robinson T, McMullan G, Marchant R, Nigam P. Remediation of dyes in textile effluent: a critical review on current treatment technologies with a proposed alternative. Bioresour Technol. 2001;77(3):247-255.
2. Forgacs E, Cserháti T, Oros G. Removal of synthetic dyes from wastewaters: a review. Environ Int. 2004;30(7):953-971.
3. Holkar CR, Jadhav AJ, Pinjari DV, Mahamuni NM, Pandit AB. A critical review on textile wastewater treatments: possible approaches. J Environ Manage. 2016;182:351-366.
4. Hoffmann MR, Martin ST, Choi W, Bahnemann DW. Environmental applications of semiconductor photocatalysis. Chem Rev. 1995;95(1):69-96.
5. Konstantinou IK, Albanis TA. TiO2-assisted photocatalytic degradation of azo dyes in aqueous solution: kinetic and mechanistic investigations: a review. Appl Catal B Environ. 2004;49(1):1-14.
6. Rauf MA, Ashraf SS. Fundamental principles and application of heterogeneous photocatalytic degradation of dyes in solution. Chem Eng J. 2009;151(1-3):10-18.
7. Akpan UG, Hameed BH. Parameters affecting the photocatalytic degradation of dyes using TiO2-based photocatalysts: a review. J Hazard Mater. 2009;170(2-3):520-529.
8. Zhang Q, Zhang K, Xu D, Yang G, Huang H, Nie F, et al. CuO nanostructures: synthesis, characterization, growth mechanisms, fundamental properties, and applications. Prog Mater Sci. 2014;60:208-337.
9. Kabra K, Chaudhary R, Sawhney RL. Treatment of hazardous organic and inorganic compounds through aqueous-phase photocatalysis: a review. Ind Eng Chem Res. 2004;43(24):7683-7696.
10. Box GEP, Wilson KB. On the experimental attainment of optimum conditions. J R Stat Soc Series B Stat Methodol. 1951;13(1):1-45.
11. Bezerra MA, Santelli RE, Oliveira EP, Villar LS, Escaleira LA. Response surface methodology (RSM) as a tool for optimization in analytical chemistry. Talanta. 2008;76(5):965-977.
12. Montgomery DC. Design and Analysis of Experiments. 8th ed. Hoboken (NJ): John Wiley & Sons; 2013.
13. Patterson AL. The Scherrer formula for X-ray particle size determination. Phys Rev. 1939;56(10):978-982.
14. Tauc J, Grigorovici R, Vancu A. Optical properties and electronic structure of amorphous germanium. Phys Status Solidi B. 1966;15(2):627-637.
15. Brunauer S, Emmett PH, Teller E. Adsorption of gases in multimolecular layers. J Am Chem Soc. 1938;60(2):309-319.
16. Derringer G, Suich R. Simultaneous optimization of several response variables. J Qual Technol. 1980;12(4):214-219.
17. Houas A, Lachheb H, Ksibi M, Elaloui E, Guillard C, Herrmann JM. Photocatalytic degradation pathway of methylene blue in water. Appl Catal B Environ. 2001;31(2):145-157.
18. Kansal SK, Singh M, Sud D. Studies on photodegradation of two commercial dyes in aqueous phase using different photocatalysts. J Hazard Mater. 2007;141(3):581-590.